

## Initial Ice Microparticle Sublimation Measurements from the Levitating Upper-Tropospheric Environmental Simulator (LUTES)

NATHAN MAGEE, KAYLA SPECTOR, YI-HSUAN LIN, COREY TONG, AND JOHN BEATTY

*The College of New Jersey, Ewing, New Jersey*

(Manuscript received 3 February 2011, in final form 12 April 2011)

### ABSTRACT

Initial ice particle sublimation data are presented from the new Levitating Upper-Tropospheric Environmental Simulator (LUTES) at The College of New Jersey. This experimental system mimics the conditions of a typical cirrus cloud in order to evaluate the phase-change kinetics of single ice particles. These ice particles are charged and then trapped in a levitating electrodynamic balance where they can be observed as they sublime in a subsaturated atmosphere. Levitation and sublimation take place within a vacuum chamber, which is contained in a freezer at a temperature of  $-40^{\circ}$  to  $-80^{\circ}\text{C}$  and is capable of a reduced pressure of 10 mb. The sublimation rates of the ice particles are observed at a variety of temperature, humidity, and pressure conditions and are compared to sublimation rates predicted by particle-scale diffusion models. Initial measurements suggest that the diffusion models are capturing the essential sublimation behavior of the particles, but further measurements promise to inform lingering questions about the fundamental thermodynamics and surface processes of sublimating and growing ice particles under cirrus conditions.

### 1. Introduction

Cirrus clouds, which form in the upper troposphere, are composed of water ice (typically ice  $I_h$ ) particles of widely variable shapes and sizes. The remote altitudes, low pressures, and low temperatures of the upper troposphere have limited in situ experimentation on cirrus particles to several types of aircraft and balloon-borne measurements (e.g., Miloshevich et al. 2006; Heymsfield et al. 2006; Monier et al. 2006; McFarquhar et al. 2007; Jensen et al. 2009; Scheuer et al. 2010). The harsh conditions have likewise restricted experimental measurements to a relatively sparse set (e.g., Shaw et al. 2000; Fukuta and Gramada 2003; Bailey and Hallett 2004; Magee et al. 2006). At temperatures between 200 and 240 K, measurements of temperature are still quite straightforward, but it becomes increasingly difficult to measure trace moisture with precision (Funke et al. 2003; Bell et al. 2004; Sayres et al. 2009; Jensen et al. 2009). Furthermore, it is essentially impossible to follow the growth or sublimation of individual particles in real

time. Observing a single particle in real time using a cirrus as a balloon or aircraft probe is necessarily capturing a single snapshot of a particle at some undefined point in its lifetime. Because of these challenges, some of the most fundamental thermodynamic parameters and physical characteristics of ice particle surfaces are still highly uncertain at cirrus-relevant temperatures and pressures. Specifically, the equilibrium vapor pressure with respect to ice  $e_{\text{sat},i}$  can vary by several percent based on which set of measurements is chosen (Murphy and Koop 2005). The latent heat of sublimation  $L_s$  is also subject to uncertainty (Cantrell et al. 2011). Furthermore, the extent to which kinetic effects may be affecting molecular dynamics at the ice surface is also an unresolved question (Gierens et al. 2003; Monier et al. 2006; Magee et al. 2006; Harrington et al. 2009).

Despite these fundamental physical uncertainties, sophisticated cloud and climate models have incorporated simulations of finescale and broadscale cirrus behaviors that are based on unverified parameterizations of particulate diffusive growth and sublimation (i.e., Harrington et al. 2009; Gierens and Bretl 2009). A broad recognition of the imperfection of these models has underscored the need to improve our understanding of the fundamental physical processes that govern cirrus evolution. For instance, there is widespread agreement that the modulation of cirrus cloud–radiation feedbacks

---

*Corresponding author address:* Nathan Magee, Department of Physics, The College of New Jersey, 2000 Pennington Rd., Ewing, NJ 08628.  
E-mail: magee@tcnj.edu

in the face of a changing climate represents one of the largest sources of uncertainty in climate models (Marquart et al. 2003; Bony et al. 2006). This concern can be illustrated by several continuing conundrums regarding cirrus cloud characterization (Kramer et al. 2009). There remains a general discrepancy between the predicted behavior and the observed behavior of cirrus clouds, which cover a wider area and sublimate more slowly than most numerical models predict (Peter et al. 2006). Furthermore, the typical concentration of very small ice crystals in cirrus clouds has been the subject of intense debate. Aircraft measurements have typically indicated much higher concentrations of small ice particles than most models would predict (Heymsfield et al. 2006; McFarquhar et al. 2007; Mitchell et al. 2008). Consensus currently appears to attribute most of these anomalous readings to measurement-induced particulate shattering (Jensen et al. 2009). On the other hand, other authors find that large numbers of small crystals are consistent with remote sensing measurements of clouds (Prabhakara et al. 1988; Garrett 2007; Cooper and Garrett 2010) and there are alternate hypotheses that might explain the real presence of high concentrations of small crystals. For instance, inhibitive surface kinetic effects due to structural (Gierens et al. 2003; Monier et al. 2006; Magee et al. 2006) or chemical effects (Scheuer et al. 2010) could slow moisture uptake and sublimation. These high concentrations of tiny ice particles, if real, would play a large part in determining the radiative impact of cirrus clouds in global climate change scenarios. The sizes of ice particles that can be effectively studied in the Levitating Upper-Tropospheric Environmental Simulator (LUTES) are included in this range (maximum dimension 5–100  $\mu\text{m}$ ) where typical cirrus concentrations are still unclear. The importance and unsettled state of continuing research in cirrus processes underscores the need for experiments and new techniques to verify and refine our picture of the physical processes operating within cirrus clouds. The focus of this research is to better understand the sublimation rates of ice under cirrus-like conditions. By comparing measured and modeled sublimation rates, it is possible to test state-of-the-art parameterizations against an imperfectly understood physical system.

## 2. The LUTES System

### a. System characteristics

The LUTES system has been constructed to incorporate active environmental control of ambient air temperature, pressure, and water vapor density. In principle, it is also possible to actively vary ambient gas composition and to introduce trace gases. The experimental system is

intended to facilitate measurements of key physical processes that are comparatively inaccessible in the upper portion of the troposphere ( $\sim 5$  to  $\sim 20$  km). The core experimental platform is in the form of a levitating quadrupole plus one electrodynamic balance (EDB; see Fig. 1). This device provides for surface-free trapping and manipulation of particles in the range of 5–100- $\mu\text{m}$  diameter (Hu and Makin 1991).

The temperature control is provided by a 17 ft<sup>3</sup> So-Low Ultra laboratory freezer. The freezer provides stable temperature control between  $-40^\circ$  and  $-80^\circ\text{C}$ . Within the freezer, a 12-in.-diameter cylindrical vacuum chamber houses the EDB platform and is outfitted with gas handling, high-voltage power, low-voltage power, temperature and pressure measurement, and optical feed-through ports.

### b. Ice particle sublimation configuration

Small (10–100- $\mu\text{m}$  diameter) ice particles can be generated for analysis in a variety of ways. For example, spraying a fine mist of water into liquid nitrogen ( $\text{LN}_2$ ) quickly generates a uniform collection of fine microspheres. The microscale surface structure of these  $\text{LN}_2$  frozen droplets is expected to deviate from ice particles grown through vapor deposition and also from droplets frozen at atmospheric temperatures (i.e.,  $-10^\circ$  to  $-40^\circ\text{C}$ ). The variation of particle genesis is one variable that will be used to evaluate the likelihood of surface kinetic effects to affect macroscopic particle sublimation behavior. Once frozen, the ice particles are sorted by microsieve to limit maximum dimension. Particles are suspended in liquid nitrogen and poured into a 75- $\mu\text{m}$  sieve, which filters out any larger particles. The challenging sorting process is expedited by placing the particle collection unit in a sieve-shaker, thus agitating the particles, and by supplying a constant stream of liquid nitrogen through the system. The presence of liquid nitrogen also serves to keep the particles at a constant temperature, isolates them from premature deposition or sublimation, and minimizes coagulation. The particles move through the sieve and accumulate in a custom-built particle collection unit. The unit consists of a shallow brass funnel that fits tightly into the microsieve housing. The ice particles move through the funnel and collect in a 3-mm-deep divot centered in a 9.5-mm-diameter removable steel collection cup. Once an adequate sample (typically several hundred particles) has been collected in the divot, the steel cup containing the ice particles is removed via cylindrical spring-loaded tongs and is then seated within a groove at the top of the charging electrode in the levitation cell (visible in Fig. 1). Exposure of the ice microparticles to room temperature air or mechanical scooping for even a few seconds can quickly

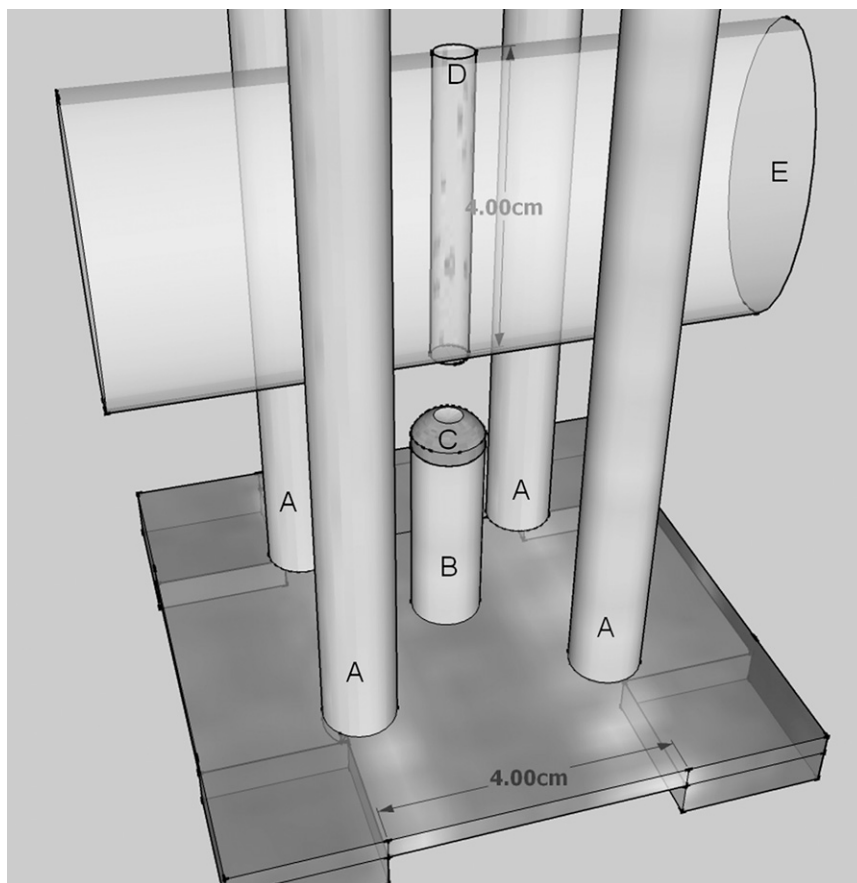


FIG. 1. Diagram of quadrupole plus one EDB including zone of levitation (thin vertical cylinder) and optical pathway for lighting and video (cylinder of elliptical cross section). The cylindrical vertical electrodes are  $\frac{3}{8}$ -in. polished stainless steel. The detachable particle collection cup is shown atop the short central electrode.

cause unwanted deposition, sticking, deformation, and melting of the ice microparticles. Our method of particle collection maintains a controlled thermal environment at all times and minimizes the handling of ice particles prior to levitation.

### c. Levitation parameters and data collection

Once the ice particles are loaded into the central electrode divot, the vacuum vessel is closed and pumped down to the experimental pressure. A gentle, continuous flow of prechilled dry nitrogen, dry air, or air/water vapor mixture flows through the EDB cell to maintain constant ambient conditions. Trace moisture measurements (Michell instruments, Easi-Dew Online) are made on this gas mixture through a shunted section of tubing after it is pulled outside of the freezer by a mechanical vacuum pump. This instrument is based on Michell's "Advanced Ceramic Moisture Sensor" technology and is capable of measuring dewpoint with stated accuracy of  $\pm 1^\circ\text{C}$  in the range of  $-100^\circ$  to  $+20^\circ\text{C}$ . The ambient

experimental temperature is determined by the temperature setting of the freezer. The freezer and steel vacuum vessel have a large thermal inertia, so temperatures during a given sublimation experiment are very stable ( $\pm 0.05^\circ\text{C}$ ) as measured by platinum resistance thermometry. A change of experimental temperature by  $10^\circ\text{C}$  requires approximately 12 h to reach a new thermal equilibrium.

The vertical electrodes of the EDB are supplied with voltages near 1000 V and a frequency of 100 Hz. Electrodes at opposite corners of the EDB are in phase and are  $180^\circ$  out of phase with the other two electrodes. The voltage parameters and electrode spacing define a dynamic saddle potential (Fig. 3). The horizontal electric field along the central vertical axis is zero, but under any horizontal deflection the potential gradient rises quickly to push a charged particle back to the center. As long as the charged particle possesses a charge-to-mass ratio in the appropriate range, confinement can be maintained indefinitely. The vertical force balance is accomplished

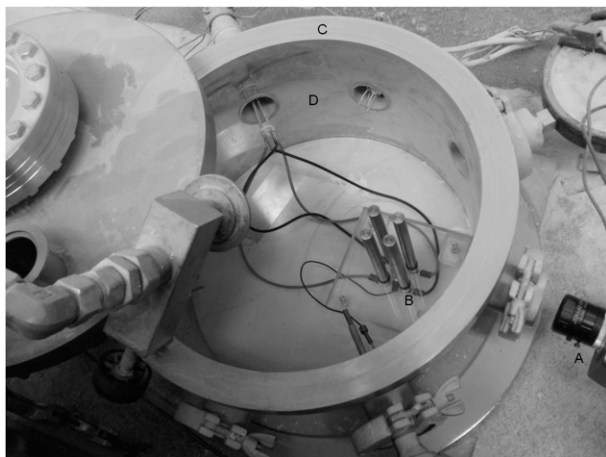


FIG. 2. The levitation cell and vacuum chamber inside the So-Low freezer.

by a dc voltage placed on the central bottom electrode. A high initial voltage of 1000–5000 V-dc is used to induce positive net charge onto the ice particles resting in the central divot and generate repulsive forces to propel these particles upward into the confining zone. Depending on the selected voltage parameters, individual particles or dozens of particles can be trapped along the axis simultaneously. Because multiparticle confinement results in repulsive particle spacing, all sublimation measurements are made on singularly trapped particles. Initial injection of ice particles often trapped several to a dozen nearly identical ice particles. Levitation frequency was then adjusted downward to select only a

narrow charge-to-mass range for stable levitation. Within several seconds, all but one particle would be ejected from levitation balance. Once a particle is trapped by the high launching voltage, the central electrode voltage is reduced (typically near 100 V-dc) to lower the particles to a position 35 mm above the central electrode surface. The vertical electric field generated by the central electrode exactly balances the weight of the particle; as the particle sublimates, the field is reduced to maintain constant particle position. This field reduction is then translated into a change in mass:

$$\frac{\Delta m}{m_0} = \frac{\Delta E}{E_0} \tag{1}$$

Changes in the voltage required to produce the balancing vertical field are easily made and recorded with high precision, resulting in excellent sensitivity to normalized changes in mass. Salt particles have been levitated for many days, indicating that any charge leakage from the surface of levitated particles is extremely slow. Advantages of the quadrupole EDB geometry over cubic geometries include much improved optical access to the levitated particle as well as a straightforward analytical solution to the bounds of stable particle confinement (Magee et al. 2006; Davis 1997; Hu and Makin 1991).

### 3. Preliminary data

Ice particle sublimation rates have been measured for LN<sub>2</sub> frozen particles at temperatures between –40° and

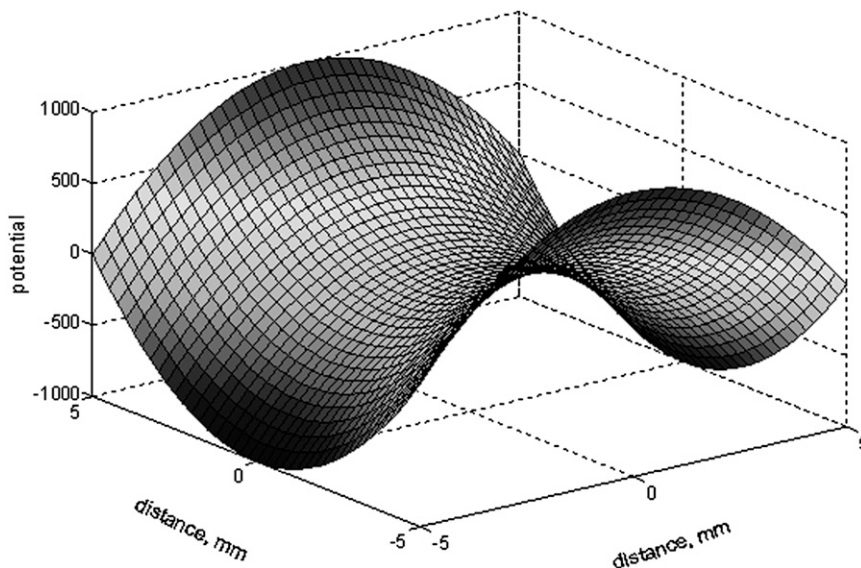


FIG. 3. Saddle AC electric potential along the horizontal plane through a levitated ice particle. For a complete theoretical treatment of the quadrupole EDB plus one levitation configuration, please see Hu and Makin (1991).

$-60^{\circ}\text{C}$  and at several pressures between 100 and 1050 mb and in subsaturated conditions between  $-0.05$  and  $-0.95 s_i$ . The mass rate of sublimation of the ice particle is modeled by

$$\frac{dm}{dt} = \frac{4\pi s_i}{\frac{RT_{\infty}}{e_{\text{sat},i} D_v^*} + \frac{L_s}{k_a} \left( \frac{L_s M_w}{RT_{\infty}} - 1 \right)}. \quad (2)$$

This expression (Pruppacher and Klett 1997, p. 547) assumes a spherical ice particle, although deviations from sphericity can be accounted for through an effective capacitance factor in the numerator. In (2),  $R$  is the ideal gas constant and  $M_w$  is the molecular weight of water. Functional parameters in (2) are  $e_{\text{sat},i}$ , the saturation vapor pressure of ice;  $L_s$ , the latent heat of sublimation;  $s_i$ , the supersaturation of the ambient air with respect to ice;  $T_{\infty}$ , the temperature of the ambient air; and  $k_a$ , the thermal conductivity of the ambient air. Please note that negative measured values of  $s_i$  discussed throughout this paper give the degree of undersaturation of the ambient air. All of the functional parameters on the right-hand side of this equation were measured directly or closely approximated for our experimental conditions. The potential effect of kinetic resistance at the ice surface is incorporated through the parameter  $\alpha$  within a modified, pressure-dependent diffusion coefficient:

$$D_v^* = \frac{D_v}{\frac{r}{r + \Delta} + \frac{D_v}{\alpha r} \sqrt{\frac{2\pi}{R_v T_{\infty}}}}. \quad (3)$$

A representative sublimation measurement is shown in Fig. 4. In this figure, circular points show sublimation of a  $\sim 60\text{-}\mu\text{m}$ -diameter ice sphere at  $-40^{\circ}\text{C}$ ,  $-0.65 s_i$ , and 250 mb. Over the course of 1 min of levitation, the ice particle loses slightly more than 70% of its initial mass; at first, the normalized sublimation occurs linearly, with some decrease in sublimation rate observed as the particle becomes smaller. The measured behavior of the ice particle and the shape of the sublimation curve appear to be well captured by the particle model (plotted curves bound experimental error). These preliminary measurements suggest that the sublimation equation and its constituent parameters, as defined by the best-accepted measurements (Murphy and Koop 2005), are indeed providing a realistic picture of ice particle sublimation. Nevertheless, the degree to which the model formulation and the values of  $e_{\text{sat},i}$ ,  $L_s$ , and  $\alpha$  (expressed within  $D_v^*$ ) can be validated by these data is presently limited by experimental uncertainties. Nelson (1998) makes an argument that the rounded shapes produced from

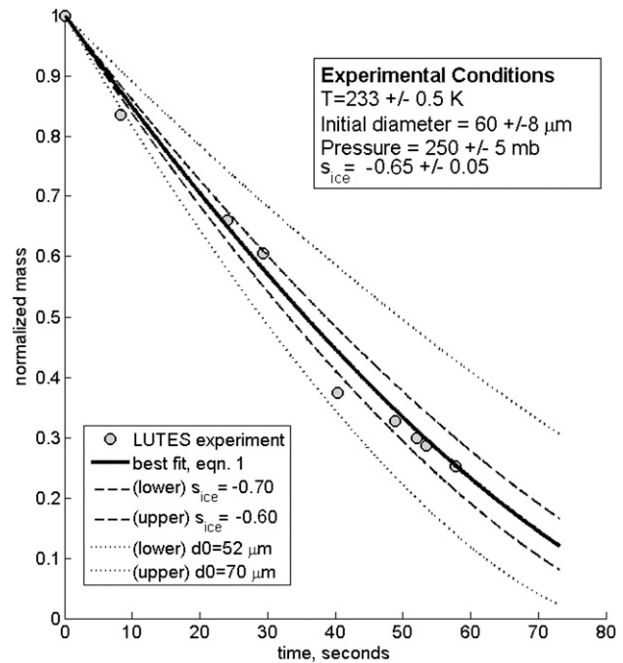


FIG. 4. Sublimation measurements of decreasing mass, normalized to the initial particle mass  $m_0$  (circles) and particle model [(2), solid line] for  $\text{LN}_2$  frozen ice particles at  $-40^{\circ}\text{C}$ . The bracketing curves express (2) given deviations in  $s_{\text{ice}}$  (dashed) and initial particle diameter (dotted).

sublimating crystal facets implies that sublimation is inherently diffusion limited and should not be significantly affected by the microscale condition of the surface, but we have not quite achieved the measurement precision required to test this assertion. Sensitivity of (3) to variations in  $\alpha_m$  are not shown in Fig. 4 because changes of a few percent in normalized mass over a time scale of minutes would not be evident in this sample. The right-hand denominator term in (3) only plays a significant role in determining the modified diffusion coefficient once the particle reaches a diameter approaching  $20\ \mu\text{m}$ ; at larger sizes the left-hand denominator term dominates and precludes a major role for  $\alpha$ . This particular sublimation event contains only two measurements at diameters below  $20\ \mu\text{m}$  so virtually no kinetic conclusions can be drawn. Further measurements in LUTES should be able to directly investigate Nelson's predictions of inherent differences between ice sublimation and growth.

#### 4. Discussion

The most significant experimental uncertainty present in the current data is related to determination of the initial particle mass ( $m_0$ ). The initial particle size can presently be controlled by the particle sieving process

and can also be modulated through tuning of the voltages in the quadrupole EDB. Nevertheless, the initial particle diameter can typically be determined to just  $\pm 8 \mu\text{m}$ . Furthermore, production of ice particles by freezing in  $\text{LN}_2$  results in highly spherical in highly spherical particles at time of launch, but we have not yet been able to capture post-levitated particles to image them for potential changes in aspect ratio. Testing for variance in sublimation behavior among shock-frozen droplets, slowly frozen droplets, single ice crystals, and polycrystals should reveal fascinating results. Some uncertainty in the environmental saturation ratio ( $s_i \pm 5\%$ ) is also present. Fundamental improvements in the LUTES experimental system are underway and include calibration of initial particle size through direct imaging, optical scattering interference measurements, application of calibration beads (Connolly et al. 2007), and inclusion of cavity ring-down spectroscopy to more accurately determine ambient moisture content [see Moyer et al. (2008) and Sayres et al. (2009) for a discussion of cavity-enhanced absorption spectrometry for water vapor]. In addition, an automated video/voltage feedback module is under development and should greatly improve the data sampling rate and more readily identify any true deviations from a smooth sublimation curve. These improvements, along with systematic variations in particle growth or freezing mechanism, should help to further validate or refine the Pruppacher and Klett sublimation formulation (2) and should cast some light on the magnitude of the latent heat of sublimation, the vapor pressure, and the kinetic deposition coefficient, all of which have relatively weak experimental basis under these conditions.

*Acknowledgments.* The authors would like to acknowledge the support of The College of New Jersey Office of Academic Affairs and Research Corporation Cottrell College Science Award 19914. Dr. Margaret Benoit, Joseph Grippaldi, and John Lenehan provided extensive technical support.

#### REFERENCES

- Bailey, M., and J. Hallett, 2004: Growth rates and habits of ice crystals between  $-20^\circ$  and  $-70^\circ\text{C}$ . *J. Atmos. Sci.*, **61**, 514–544.
- Bell, S. A., T. Gardiner, R. M. Gee, M. Stevens, K. Waterfield, and A. Wooley, 2004: An evaluation of performance of trace moisture measurement methods. National Physical Laboratory Report, Teddington, United Kingdom. [Available online at <http://www.tigeroptics.com/pdf/Paper064NPL.pdf>]
- Bony, S., and Coauthors, 2006: How well do we understand and evaluate climate change feedback processes? *J. Climate*, **19**, 3445–3482.
- Cantrell, W., A. Kostinski, A. Szedlak, and A. Johnson, 2011: Heat of freezing for supercooled water: Measurements at atmospheric pressure. *J. Phys. Chem.*, **115**, 5729–5734, doi:10.1021/jp103373u.
- Connolly, P., M. Flynn, Z. Ulanowski, T. W. Chourlatan, M. Gallagher, and K. N. Bower, 2007: Calibration of the cloud particle imager probes using calibration beads and ice crystal analogs: The depth of field. *J. Atmos. Oceanic Technol.*, **24**, 1860–1879.
- Cooper, S. J., and T. J. Garrett, 2010: Identification of small ice cloud particles using passive radiometric observations. *J. Appl. Meteor. Climatol.*, **49**, 2334–2347.
- Davis, E. J., 1997: A history of single aerosol particle levitation. *Aerosol Sci. Technol.*, **26**, 212–254.
- Fukuta, N., and C. M. Gramada, 2003: Vapor pressure measurement of supercooled water. *J. Atmos. Sci.*, **60**, 1871–1875.
- Funke, H. H., B. L. Grissom, C. E. McGrew, and M. W. Raynor, 2003: Techniques for the measurement of trace moisture in high-purity electronic specialty gases. *Rev. Sci. Instrum.*, **74**, 3909–3933.
- Garrett, T. J., 2007: Comments on “Effective radius of ice cloud particle populations derived from aircraft probes.” *J. Atmos. Oceanic Technol.*, **24**, 1495–1503.
- Gierens, K. M., and S. Bretl, 2009: Analytical treatment of ice sublimation and test of sublimation parameterisations in two-moment ice microphysics model. *Atmos. Chem. Phys.*, **9**, 7481–7490.
- , M. Monier, and J.-F. Gayet, 2003: The deposition coefficient and its role for cirrus clouds. *J. Geophys. Res.*, **108**, 4069, doi:10.1029/2001JD001558.
- Harrington, J. Y., D. Lamb, and R. Carver, 2009: Parameterization of surface kinetic effects for bulk microphysical models: Influences on simulated cirrus dynamics and structure. *J. Geophys. Res.*, **114**, D06212, doi:10.1029/2008JD011050.
- Heymsfield, A. J., C. Schmitt, A. Bansemer, G. J. van Zadelhoff, M. J. McGill, C. Twohy, and D. Baumgardner, 2006: Effective radius of ice cloud particle populations derived from aircraft probes. *J. Atmos. Oceanic Technol.*, **23**, 361–380.
- Hu, D., and B. Makin, 1991: Study of a five-electrode quadrupole levitation system; Theoretical aspects. *IEE Proc.*, **138A**, 320–336.
- Jensen, E. J., and Coauthors, 2009: On the importance of small ice crystals in tropical anvil cirrus. *Atmos. Chem. Phys.*, **9**, 5519–5537.
- Krämer, M., and Coauthors, 2009: Ice supersaturations and cirrus cloud crystal numbers. *Atmos. Chem. Phys.*, **9**, 3505–3522.
- Magee, N., A. M. Moyle, and D. Lamb, 2006: Experimental determination of the deposition coefficient of small cirrus-like ice crystals near  $-50^\circ\text{C}$ . *Geophys. Res. Lett.*, **33**, L17813, doi:10.1029/2006GL026665.
- Marquart, S., M. Ponater, F. Mager, and R. Sausen, 2003: Future development of contrail cover, optical depth, and radiative forcing: Impacts of increasing air traffic and climate change. *J. Climate*, **16**, 2890–2904.
- McFarquhar, G. M., J. Um, M. Freer, D. Baumgardner, G. L. Kok, and G. Mace, 2007: Importance of small ice crystals to cirrus properties: Observations from the Tropical Warm Pool International Cloud Experiment (TWP-ICE). *Geophys. Res. Lett.*, **34**, L13803, doi:10.1029/2007GL029865.
- Miloshevich, L. M., H. Vömel, D. N. Whiteman, B. M. Lesht, F. J. Schmidlin, and F. Russo, 2006: Absolute accuracy of water vapor measurements from six operational radiosonde types launched during AWEX-G and implications for AIRS validation. *J. Geophys. Res.*, **111**, D09S10, doi:10.1029/2005JD006083.
- Mitchell, D. L., P. Rasch, D. Ivanova, G. McFarquhar, and T. Nousiainen, 2008: Impact of small ice crystal assumptions on ice sedimentation rates in cirrus clouds and GCM simulations. *Geophys. Res. Lett.*, **35**, L09806, doi:10.1029/2008GL033552.

- Monier, M., W. Wobrock, J.-F. Gayet, and A. Flossmann, 2006: Development of a detailed microphysics cirrus model tracking aerosol particles' histories for interpretation of the recent INCA campaign. *J. Atmos. Sci.*, **63**, 504–525.
- Moyer, E. J., D. S. Sayres, G. S. Engel, J. M. St. Clair, F. N. Keutsch, N. T. Allen, J. M. Kroll, and J. G. Anderson, 2008: Design considerations in high-sensitivity off-axis integrated cavity output spectroscopy. *Appl. Phys.*, **92B**, 467–474.
- Murphy, D., and T. Koop, 2005: Review of the vapour pressures of ice and supercooled water for atmospheric applications. *Quart. J. Roy. Meteor. Soc.*, **131**, 1539–1565.
- Nelson, J., 1998: Sublimation of ice crystals. *J. Atmos. Sci.*, **55**, 910–919.
- Peter, T., C. Marcolli, P. Spichtinger, T. Corti, M. Baker, and T. Koop, 2006: When dry air is too humid. *Science*, **314**, 1399–1402.
- Prabhakara, C., R. S. Fraser, G. Dalu, M.-L. C. Wu, R. J. Curran, and T. Styles, 1988: Thin cirrus clouds: Seasonal distribution over oceans deduced from Nimbus-4 IRIS. *J. Appl. Meteor.*, **27**, 379–399.
- Pruppacher, H. R., and J. D. Klett, 1997. *Microphysics of Clouds and Precipitation*. Kluwer Academic, 954 pp.
- Sayres, D. S., and Coauthors, 2009: A new cavity based absorption instrument for detection of water isotopologues in the upper troposphere and lower stratosphere. *Rev. Sci. Instrum.*, **80**, 044102, doi:10.1063/1.3117349.
- Scheuer, E., J. E. Dibb, C. Twohy, D. C. Rogers, A. J. Heymsfield, and A. Bansemer, 2010: Evidence of nitric acid uptake in warm cirrus anvil clouds during the NASA TC4 campaign. *J. Geophys. Res.*, **115**, D00J03, doi:10.1029/2009JD012716.
- Shaw, R., D. Lamb, and A. M. Moyle, 2000: An electrodynamic levitation system for studying individual cloud particles under upper-tropospheric conditions. *J. Atmos. Oceanic Technol.*, **17**, 940–948.